

Evaluation of the Suitability of Natural Flower Dyes Spectra on Dye-Sensitized Solar Cell (DSSC) Containing TiO_2 and I^-/I_3^- With Respect to Stability and Efficiency

Aseel Mohammed Ali Zakar , Salah A. Naman, and Sabah M. Ahmed

Abstract—Different dye-sensitized solar cells (DSSC) were fabricated using TiO_2 as a semiconductor with two groups of flowers, nursery flowers from Duhok city and mountain flowers. The ultraviolet (UV)-visible absorption spectra of these dyes were examined. Current density–voltage (J–V) characteristics for each fabricated cell were recorded at ambient temperature. The stability of these cells has been examined through annealing time. The mountain flower dyes have been collected from Gara Mountain at a height about 2500 m above sea level for which they are believed to have resistivity to UV light. The efficiencies of the cells mostly depend on the visible absorption of the dye while their stabilities depend on the ultraviolet absorption of these dyes. As a compromise, the nursery flower dyes efficiencies were between 1.88% and 4.19%, while mountain flowers were between 1.83% and 4.82%. Although we get low efficiency in comparison to other workers, however, in this study we are after getting the best stability of natural flower dyes. The current findings are substantially added to our understanding of the stability of DSSC. Some suitable stable natural flowers were selected for our new program of DSSC research. The statistical *P* values show that the efficiencies of mountain flower dyes are much more stable than that of nursery flower dyes.

Index Terms—Dye-sensitized solar cells (DSSC), Current density–voltage (J–V) characteristics, efficiency, natural flower dyes, ultraviolet (UV)-Visible absorption spectra.

I. INTRODUCTION

SOLAR energy conversion to electricity has been done for a long time. Different methods are being advanced to convert the light to electricity using liquid junction photovoltaic cells [1] or using the different organic molecules as in a photo galvanic cell and photoelectrochemical cells [2], and organometallic

complexes [3] in late 1970–1990 as in a dye-sensitized solar cell (DSSC) of Grätzel. He had used an organometallic complex similar to chlorophyll which he calls photosensitized solar cell, DSSC. Recently, the improvement of the efficiency of dyed monocrystalline silicon solar cells by covering them with natural plant pigments has been done in our lab [4]. In the late 1960s, the researchers generated electricity from illuminated organic dyes in electrochemical cells [5]. Later, many years of unremitting efforts in improving the efficiency of DSSC were spent since the amount of energy provided by the sun in one hour is huge and much more the consumption by the human in one year. Then in 1991, Grätzel made a breakthrough when he introduced a titanium dioxide semiconductor to increase the light-harvesting getting 7% efficiency and called these cells DSSC [6]–[8]. The field is growing fast, and the cells of 11% efficiency are reachable [9], [10]. In 2013, Grätzel announced a 15.0% efficiency of Solid State DSSC [11].

Economic as well as nontoxic and environmentally friendly aspects of DSSC make it one of the most promising types of photovoltaic cells for the conversion of light energy to electricity.

The DSSC which is the subject of this research was experimented by O'Regan and Grätzel [12]. It consists of an organic-based photovoltaic cell as a dye-sensitized semiconductor material, often titanium dioxide TiO_2 , where the dye molecule attached to the semiconductor acts as a light absorber.

Under illumination, many processes play an important role in converting the light energy to electricity. Since the dye molecule (D) is sensitive to the light, it is easily excited by light energy resulting in an unstable sensitizer molecule (D^*) in the lowest unoccupied molecular orbital (LUMO) band as shown in reaction (1) and Fig 1. To be stable and in an ideal condition, a photocurrent electron is released by the excitation molecule which injects into the conduction band (CB) in the semiconductor yielding a sensitizer hole (D^+) as shown in reaction formula (2). Next, the photoelectrons in CB as in reaction (3) reach the counter electrode (CE) through an external circuit as illustrated in reaction (4). With the help of the electrons that come from the CE, dye at an excited state is reducing some of its oxidation energy in the electrolyte. This led to Red according to reaction (5). Finally, as in the reaction formula (6), D^+

Manuscript received January 17, 2021; accepted February 22, 2021. Date of publication March 29, 2021; date of current version April 21, 2021. This work was supported by the Dr Ahmed Family Pty Ltd, New South West, Australia supplies us with SMU 2450-Keithley. (Corresponding author: Aseel Mohammed Ali Zakar.)

Aseel Mohammed Ali Zakar is with the Department of Physics, College of Science, University of Duhok, Kurdistan 42001, Iraq (e-mail: aseel.zakar@uod.ac).

Salah A. Naman is with the Department of Chemistry, Faculty of Science, University of Zakho, Kurdistan 42001, Iraq (e-mail: salah.naman@yahoo.com).

Sabah M. Ahmed is with the Department of Physics, college of Science, University of Duhok, Kurdistan 42001, Iraq (e-mail: sabma62@uod.ac).

Color versions of one or more figures in this article are available at <https://doi.org/10.1109/JPHOTOV.2021.3063017>.

Digital Object Identifier 10.1109/JPHOTOV.2021.3063017

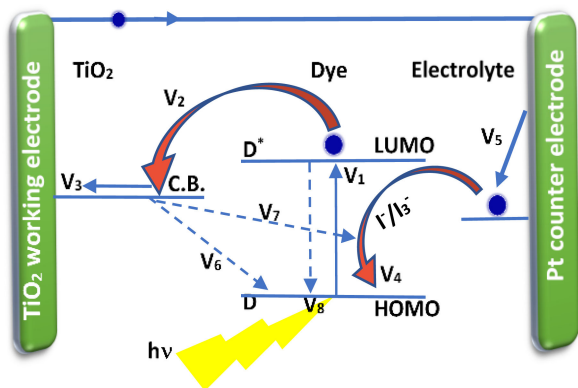
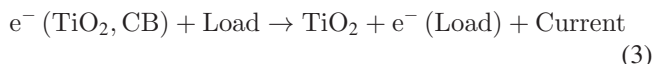
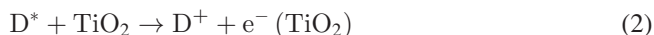


Fig. 1. Construction of DSSC cell with dye molecules based on TiO₂ semiconductor and I⁻/I₃⁻ electrolyte. The dye absorbs light radiation and releases photo-excited electrons from HOMO to LUMO at V₁, which is supposed to be injected into the conduction band (CB) in the semiconductor at V₂; at V₃ the excited electron reaches the anode through an external circuit, yielding a sensitizer hole which is regenerated by electron donation from iodide in the electrolyte at V₄, now this iodide must be regenerated by reduction process of triiodide on the counter electrode at V₅ on the cathode. Recombination at the oxide/dye interface at V₆ and electrolyte/oxide interface at V₇ besides a relaxation of the excited dye to its ground state at V₈ also occurs.

is regenerated by Red. However, the disadvantage that occurs in these processes is that they accompanied with electron-hole recombination processes as shown in reaction formulae (6)–(8) that significantly decreased the efficiency of solar cells [13], [14].



In this study, the DSSC was fabricated with natural plant dyes. The extraction process was simple and it is done with primitive tools. This study did not use Ruthenium-based, organometallic material, or any other artificial dyes which are expensive and mostly highly toxic.

II. EXPERIMENTAL PART

A. Synthesis of Natural Dye Sensitizer

This study seeks simplicity and relying on what is available in nature to get electricity. Generally speaking, all-natural dyes could be used in DSSC as sensitizers, but not all of them provide us the same stability and efficiency in converting light to electricity. For this, two groups of flowers are selected in this study for the comparison process. The first group consists

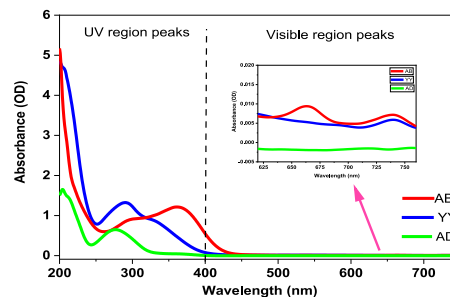


Fig. 2. UV-Visible region peaks in the absorption spectrum of Gara mountain dyes up to several units of optical density (OD) in absorbance for flower dyes AB, YY, AD, considering that each of these flowers contains a higher concentration of dyes.

of natural dyes from different special flowers at the top of Gara Mountain which is about 2500 m above sea level in the Kurdistan region, north of Iraq. They were used as sensitizers and sunlight harvesters. They are considered having a high resistivity to UV light. The second group of flowers are selected from a nursery at Duhok city (maybe some of them also originally from mountain). The extraction process was done in primitive ways either by squishing the flower or by using different solvents to extract the dyes. The process is done using the same weight of flowers and the same volume of different solvent that does not affect the color of the flower or cause degradation of pigments. However, it was difficult to match them because not all of them are soluble in the same solvent. As we are after the UV-visible spectra, the dyes were subjected to 6800 UV/Visible spectrophotometer (JENWAY, China, QA in the UK) to understand the light response of these different dyes. It is believed that these wavelengths will serve us in achieving two goals. The first goal which is the main goal from this study is that the UV spectra wavelength is thought to support stability, while the visible spectra wavelength is believed will support efficiency as it is the second goal. For example, the collection of some of these dyes' spectra is shown in Fig. 2.

Despite using the same weight of flowers in the same volume of different appropriate solvents, the spectra of these give us different optical densities (OD) as a function of different wavelengths beside different concentrations of dyes in each flower, see the following equation:

$$\text{OD} = \varepsilon LC \quad (9)$$

where ε is the extinction coefficient of dye molecules in each flower, L is the path length of the cell in cm, and C is the concentration of dye in molar.

The maximum absorbance for some of them reached up to 4 OD, while for the others, it reaches several tenths of the unit as shown in Figs. 2 and 3.

The code, the name, and the photo of each flower are illustrated in Appendix 1 [15]–[17]. The absorbance peaks at UV and visible regions for each flower are recorded in Table I.

B. Materials

Transparent titania paste, TiO₂ with 20 nm average diameter of the nanoparticle (paste A), Titania paste, reflector TiO₂ with

TABLE I
OPTICAL DENSITY (OD) OF UV-VISIBLE SPECTRA FOR GARA MOUNTAIN FLOWERS AND NURSERY CITY FLOWERS WITH THEIR NAMES AND CODS

Group of Flowers	Scientific Name of flowers	Cod of flowers	UV wavelengths		Visible wavelengths		
			λ_{\max} (nm)	Abs. (OD.)	λ_{\max} (nm)	Abs. (OD)	
Gara mountain flower dyes	<i>Paeonia officinalis</i> subsp. <i>Villosa</i>	AD	206	1.7599			
			218	1.2749			
			276	0.6761			
			359	0.0474			
	<i>Malva moschata</i> alba	YY	210	4.6216	740	0.0063	
			290	1.402			
			321	0.9347			
	<i>Hypericum thymopsis</i>	XX	356	0.9171	447	0.1057	
					590	0.1013	
	<i>Helichrysum</i> schwefellicht	AB	364	1.2334	664	0.0104	
					740	0.0075	
	<i>Achillea filipendulina</i>	WW YELLOW	345	0.1586	443	0.0378	
					470	0.0308	
		WW GREEN	340	0.3049	407	0.1207	
503					0.0182		
532					0.0158		
560					0.0099		
Nursery Duhok city flower dyes	<i>Colutea arborescens</i> , Bladder senna -	ZZ	266	0.0633	415	0.0218	
			316	0.0391			
			328	0.0335	443	0.0232	
			341	0.0368			
			352	0.0324	472	0.0196	
			372	0.0321			
	385	0.027					
	<i>Tansy</i> (<i>Tanacetum vulgare</i>)	VV	---	---	417	0.0276	
					443	0.0337	
					470	0.0286	
	<i>primula veris</i> 'Cowslips'	TT	381	0.0207	443	0.0422	
					470	0.0346	
					497	0.0024	
	<i>Petunia</i> 'Fanfare Deep Blue'	FF		252	0.8465	583	0.0076
268				0.9596			
279				0.8226			
295				0.8792			
354				0.6192			
<i>Narcissus pseudonarcissus</i>		HH		220	5.0789	424	0.2844
				254	2.3101	445	0.2179
				294	1.2356		
				353	1.5802		
<i>Calendula officinalis</i>		AA		205	5.1061		
				255	0.9651		
				341	0.6772		
				353	0.6829		
				340	0.6772		
					353	0.6818	
<i>Osteospermum ecklonis</i>		RR	328	0.1491	445	0.1628	
					472	0.1360	
<i>Calendula</i> Pot Marigold		CC	255	0.2273	422	0.2756	
	446				0.2657		
<i>Gazania rigens</i> Orange	BB		282	0.4807	445	1.509	
			330	0.3277			
			340	0.3572	467	1.5409	
			352	0.3288			
<i>Viola pedunculata</i> yellow pansy	II		258	0.2099	411	0.0741	
			300	0.0886	440	0.0847	
			365	0.1662	467	0.0707	
			381	0.14			
<i>Gazania rigens</i> Yellow	SS		250	0.5773	417	0.8473	
			269	0.5787	439	1.1782	
			299	0.6863	467	1.0461	
			328	0.7906			

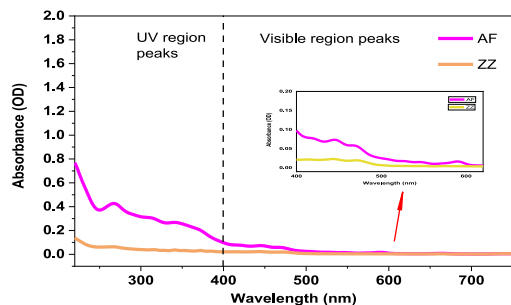


Fig. 3. UV-Visible region peaks in the absorption spectrum of Gara mountain dyes up to several tenths OD of absorbance for flower dyes AF and ZZ considering that each of these flowers contains a lower concentration of dyes.

150–250 nm average particle size (paste B) were used as working electrode layers, EL-HPE high-performance electrolyte was used as the transport for redox mediator between two electrodes, platinum paste, Pt with a highly transparent layer and high electrocatalytic activity to provide good transparency and high catalytic activity for the electrochemical reduction of I₃⁻ to I⁻ which is used as a counter electrode layer, fluorine-doped tin oxide coated glass slide FTO of surface resistivity equal to $\sim 7 \Omega/\text{sq}$, and 2.2 mm thickness, 80%–82% (visible) transmittance was used as a conducting glass, act as substrates depositing for both TiO₂ films and platinum electrodes. All these material were purchased from Sigma Aldrich, USA, and used without any further purification.

C. Preparation of the Working Electrodes

Two types of TiO₂ paste—transparent TiO₂ (paste A) and reflector microcrystalline TiO₂ (paste B) were deposited by the doctor blade method manually, forming respectively the transparent and the light-scattering layers of the photoanode electrode.

During the sintering process of the TiO₂ layer, iron cations should be removed from the surface for it enhances charge recombination in photocells [18] and quenches the dye-sensitized photocurrent (J_{sc}) effectively, beside the J_{sc} decreased by 30% upon the addition of 400 ppm Fe₂O₃ [19], [20].

To prepare the DSSC working electrodes, the FTO conductive glass was cut in area $2 \times 2 \text{ cm}^2$ and was washed with a detergent solution using an ultrasonic bath for 20 min and then rinsed with distilled water and ethanol to remove organic pollutants and iron contamination before use. Paste A was coated on the FTO glass plates by the doctor blade method. To avoid surface irregularity, the glass is kept in a clean box for 40 min relaxation time. Then dried for 6 min at 125 °C [21]. Then one layer of the same area and 10–15 μm thickness of light-scattering anatase TiO₂ film (paste B) were coated by the doctor blade method. Two different geometrical sizes, 0.28 and 0.19 cm², of the TiO₂ electrodes were used; however, the real size was 0.04 cm². After fabricated the cells, we get a different arbitrary geometrical area of our devices. So, a suitable mask of 0.04 cm² area for each device is used to let the light fall only on a certain area which is the area of the mask during measuring the energy conversion efficiency under illumination and this is the active area. In other

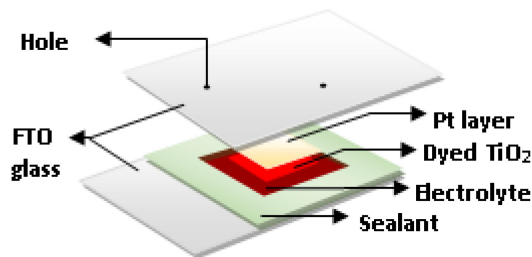


Fig. 4. Sandwich-like structure for DSSC.

words, the active area is defined by the mask area, not the TiO₂ area, and 20–24 μm thickness. The electrode coated with the TiO₂ pastes were gradually heated under an airflow at 325 °C for 5 min, at 375 °C for 5 min, and at 450 °C for 15 min, and finally, at 500 °C for 15 min [21]. After cooling to 80 °C, the TiO₂ electrode was immersed into flower dyes for about 20 h at room temperature.

D. Preparation of the Pt-Counter Electrode

First of all, two holes of 1-mm diameter on the FTO surface were drilled by a diamond drill. The FTO conductive glass was washed with ethanol and distilled water. Based on the doctor blade method, a platinum counter electrode was prepared by coating the FTO glass substrate with platinum paste. First, dry at 80 °C, and then sintered at 450 °C for 30 min with a thickness equal to the thickness of the scotch tape.

E. Electrolyte

EL-HPE High-Performance Electrolyte, Sigma Aldrich, USA, is used in this study because it has a low viscosity, high ionic conductivity liquid electrolyte (16.5–18.5 mS/cm at 20 °C), and, therefore, provides the highest performance [22].

F. Assembly of the DSSC

The working TiO₂ electrode and Pt-counter electrode were assembled into a sandwich-like structure (see Fig. 4). A hot-melt sealant was put between two electrodes, with inner dimensions 2-mm larger than the TiO₂ layer. The electrolyte was injected between the two electrodes through the holes in the back of the CE. Then, the two holes were sealed by silver tape and silicon glue to prevent evaporation.

G. Apparatuses and Instruments

In this study four prop computerized graphical interface Source-Measure Unit (SMU) 2450 - KEITHLEY is used to provide J–V curves. The intensity of the beam of light is measured by Voltcraft PL-110SM Solar Light Meter.

Fig. 5 shows Model 2450 SourceMeter connections to a solar cell. A new MATLAB R2016a program with KickStart Measurement Software is designed to be capable of auto measuring current density–voltage (J–V) curves and all other needed physical properties.

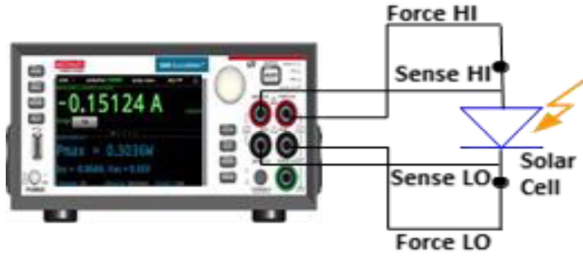


Fig. 5. Model 2450 - KEITHLEY SourceMeter connections to a solar cell.

H. Photovoltaic Outdoor Measurements

In this study, we considered outdoor photovoltaic measurements at noon with light intensity between 700 and 800 W/m². J–V characteristics were obtained by using a Keithley Model 2450 SourceMeter SMU which can source and measure both current and voltage simultaneously. The voltage step was 10 mV and the delay time of photocurrent was 40 ms.

III. RESULTS AND DISCUSSION

The absorption spectra and the J–V curves of all cells were plotted. Many cell parameters such as open-circuit voltage (V_{OC}), short circuit current density (J_{SC}), maximum power point (P_{max}), fill factor (FF), efficiency (η), and wavelength at the maximum optical density (λ_{max}) are measured according to the following mathematical equations:

$$J_{SC} = \frac{I_{SC}}{A} \quad (10)$$

where J_{SC} is the current per unit active area A of the device when the open-circuit voltage across the device is zero, I_{SC} is the maximum current available from a solar cell, and this occurs at zero voltage.

$$\eta = \frac{P_{max}}{P_{in}} \cdot 100\% \quad (11)$$

$$FF = \frac{P_{max}}{P_{theo}} = \frac{V_{MP} \cdot I_{MP}}{V_{OC} \cdot I_{SC}} \quad (12)$$

where P_{max} is the maximum generated power, P_{in} is the electrical input power from the light source, P_{theo} is the theoretical power maximum of a solar cell, V_{MP} and I_{MP} are potential and current of the I–V curve when the generated power is at the maximum, V_{OC} is the maximum voltage available from a solar cell, and this occurs at zero current.

A. Optical Properties of Dyes

The spectra of the Gara mountain flower dyes and nursery Duhok city flower dyes are plotted in Figs. 6(a) and (b) and 7, respectively. The absorption peaks of the spectra for all extracts were tabulated in Table I.

B. Photovoltaic Performance of the DSSC

To investigate the effect of the dyes on the efficiency of DSSC, all the cells were treated and fabricated under the same

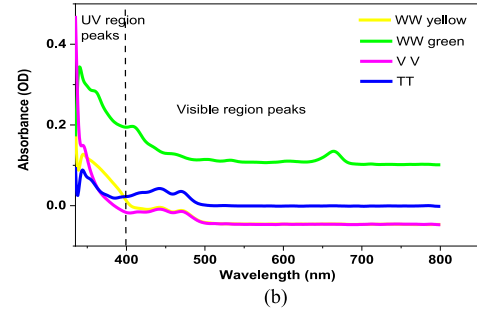
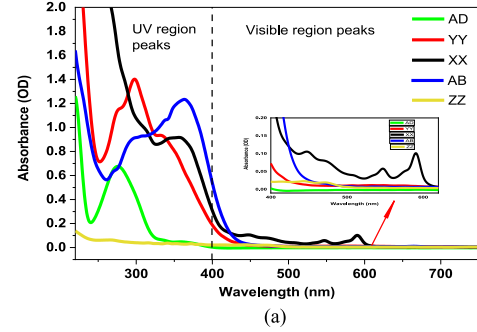


Fig. 6. Absorption spectrum of Gara mountain dyes at a different rate of absorbances for the same weight of flower leaves (0.025 gm) in the same volume of solvents (10 ml). (a) AD, YY, XX, AB, and ZZ flowers. (b) VV, TT, WW green, and WW yellow. The scales of OD in (a) and (b) are different due to different concentrations of dyes in these flowers.

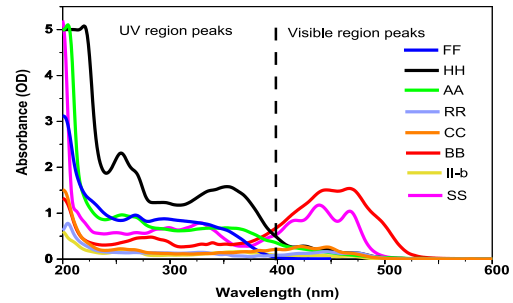


Fig. 7. Absorption spectrum of nursery Duhok city flower dyes at a different rate of absorbances for the same weight of flowers on the curve in the same volume of solvents.

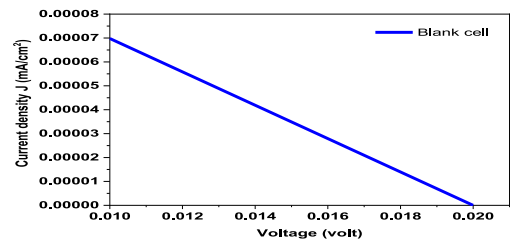


Fig. 8. Photocurrent-voltage for blank solar cells without using any sensitized dye molecule.

conditions, so having the same microstructure is what could be regarded. All cells were tested under outdoor irradiation with solar intensity ~ 400 W/m² at the noon by using neutral filtration. The current–voltage sweeps were run with the Keithley Model 2450 SourceMeter SMU and MATLAB R2016a program. The voltage sweep was from 0.00 to V_{OC} .

TABLE II
PHOTOVOLTAIC CHARACTERISTICS OF DSSC BASED ON VARIOUS TYPES OF FLOWERS FOR GARA MOUNTAIN AND NURSERY

Type of group	Cod of flowers	J _{SC} mA/cm ²	V _{OC} volt	P _{MAX} × 10 ⁻⁵ Watt	FF	η%
Gara mountain flower dyes	Blank	0.41	0.02	0.03	0.78	0.02
	AD	2.42	0.55	2.92	0.59	1.83
	YY	2.21	0.63	3.12	0.60	1.95
	XX	2.78	0.55	3.54	0.61	2.21
	WW yellow	3.54	0.49	3.87	0.58	2.42
	WW green	3.39	0.56	4.31	0.60	2.70
	AB	3.57	0.65	5.11	0.59	3.20
	ZZ	3.39	0.68	5.23	0.61	3.27
Nursery Duhok city flower dyes	VV	4.59	0.63	6.48	0.59	4.05
	TT	5.21	0.63	7.71	0.61	4.82
	FF	3.54	0.48	3.01	0.46	1.88
	HH	5.10	0.44	3.61	0.41	2.26
	AA	5.63	0.54	5.58	0.57	2.97
	RR	5.37	0.47	4.38	0.44	2.74
	CC	7.09	0.48	4.94	0.38	3.09
	BB	6.33	0.45	5.04	0.45	3.15
II	7.05	0.52	6.08	0.42	3.80	
SS	7.33	0.51	6.70	0.49	4.19	

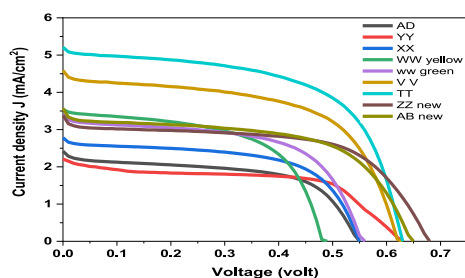


Fig. 9. Photocurrent-voltage curve of DSSC covered with different mountain flowers. The code and name of these flowers are in Table I while the IV characteristics are tabulated in Table II.

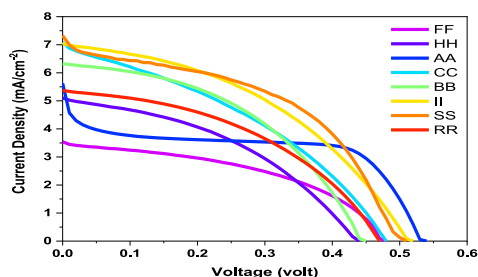


Fig. 10. Photocurrent-voltage curve of DSSC covered with different nursery flowers. The code and name of these flowers are in Table I while the IV characteristics are tabulated in Table II.

Fig. 8 shows the J–V curve of the test cell without any dye. While the J–V curves of the dye-sensitized test cells with Gara mountain and nursery city groups of dyes are illustrated in Figs. 9 and 10, respectively.

J–V sweeps show that when a TiO₂ working electrode was used without dye, the V_{OC} was only 0.02 V, the J_{SC} was 0.41 mA·cm⁻², and the η achieved was only 0.02%, as described in Table II. The reason behind such low efficiency comes from the absence of the dynamic parameter, dye-sensitized molecules. Indeed, the functioning of DSSC significantly depends on the

role of dye sensitizer molecule (in UV and visible absorbance) on the surface of semiconductor materials such as TiO₂, SnO₂, Nb₂O₅ [23], that is, the dye naturally has an ability to absorb light, paving the way of working as an electron pump to excite an electron to the LUMO where it will be injected into the CB of the semiconductor, receiving an electron from the charge mediator such as iodide/triiodide redox couple, and repeat the cycle [24], as has been mentioned earlier in reactions (1)–(8) and Fig. 1.

On the other hand, the results show that the efficiency of the DSSC with dye-covered TiO₂ electrode was increased significantly in both flower groups. In the Gara mountain group, the efficiency is ranged from 1.83% for AD dye to 4.82 for TT dye while in nursery city flower the efficiency is ranged from 1.88% for FF dye to 4.19 for SS dye. Although the nursery flowers have a better spectrum than the Gara flowers, the results show that Gara flower efficiencies are higher as in Table II.

J–V characteristic curves for the first readings (T = 0) of all samples show that the highest short circuit current density J varies from 2.21 mA/cm² for YY dye to 5.21 mA/cm² for TT dye in Gara mountain flowers, and from 3.54 mA/cm² for FF dye to 7.33 mA/cm² for SS dye in nursery flowers at Duhok city. The open-circuit voltage varies from 0.49 volt for WW yellowish color dye to 0.68 volts for ZZ dye in Gara mountain flowers, and from 0.44 volt for HH dye to 0.54 volt for AA dye in nursery flowers at Duhok city as shown in Figs. 9 and 10.

C. Statistical Analysis

The study has gone some way towards enhancing our understanding of the stability of cell efficiency. The two groups of flowers have been examined in the same period, T1 and T2, to know the differences in their stability at certain periods. Nine from the mountain group and eight from the city nursery group.

T-test paired two samples for means are applied in the range of visible band absorption because it is this band that effects

TABLE III
EFFICIENCIES AT DIFFERENT PERIODS WITH P -VALUE FOR BOTH NURSERY
AND GARA MOUNTAIN DYE FLOWERS

Cod of Mountain Flowers	$\eta\%$ T0=0 day	$\eta\%$ T1=12 days	$\eta\%$ T2=70 days
AD	1.83	1.84	1.88
YY	1.95	1.94	1.93
XX	2.21	2.22	2.18
AB	3.20	3.27	3.16
WW yellow	2.42	2.47	2.42
WW green	2.70	2.76	2.72
ZZ	3.27	3.29	3.25
VV	4.05	4.03	4.05
TT	4.82	4.54	4.52
FF	1.88	1.91	1.64
HH	2.26	2.23	2.24
AA	2.97	2.81	2.84
P-value		0.339	0.075

** In statistics, t -tests are a type of hypothesis test that allows you to compare means.

The significance level, also denoted as alpha or α , is the probability of rejecting the null hypothesis when it is true. For example, a significance level of P -value 0.05 indicates a 5% risk of concluding that a difference exists when there is no actual difference.

TABLE IV
EFFICIENCIES AT DIFFERENT PERIOD WITH P -VALUE FOR
NURSERY DYES FLOWERS

Cod of Nursery Flowers	$\eta\%$ T1=0 day	$\eta\%$ T2=12 days	$\eta\%$ T3=70 days
RR	2.74	2.13	0.63
CC	3.09	2.19	0.915
BB	3.15	2.24	1.24
II	3.80	3.34	3.17
SS	4.19	3.62	2.04
P-value		0.002	0.004

the efficiency. According to Table III, the P -value for mountain flowers was 0.339 after 12 days and 0.075 after 70 days which are much more than 0.05. This revealed that there is no significant difference in the efficiencies within the specific time and the dyes are stable as well to some extent. However, for the nursery flowers the P -values were 0.002 and 0.004 at 12 days and 70 days respectively, as in Table IV. Since they are less than 0.05, this means that their efficiencies are not stable. The reason behind the stability of efficiencies in Gara mountain flowers is counted to the existence of UV radiation at the top of the mountain where the flowers were adapted to grow in. It is obvious that the UV intensity is much more at a higher altitude, so, whatever plant grows there should have some resistivity to change to stay alive as much as possible. Regarding this fact, it is believed that there is a significant relationship between the mountain plants which have absorbance peaks at UV band and the stability of their efficiencies as described in Tables III and IV.

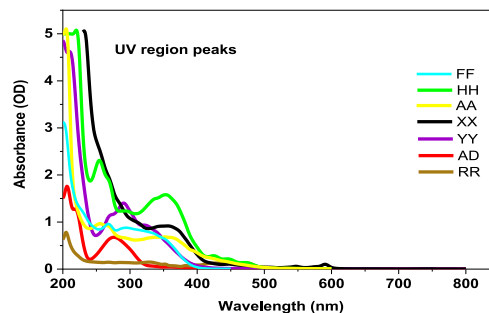


Fig. 11. UV absorbance peaks of flower dyes from both Gara Mountain and nursery groups.

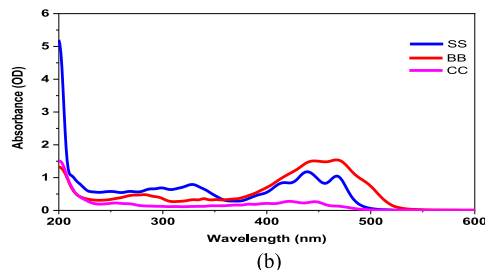
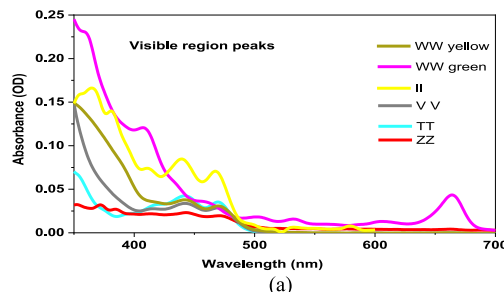


Fig. 12. (a) and (b) Visible absorbance peaks of flower dyes from both Gara Mountain and nursery groups.

IV. CONCLUSION

In our previous work, we focus on improving the efficiency of Si solar cells using natural flower dyes [4], while in this work we are after searching for the desired natural dyes that give the best stability to the cell as this is the main goal of our study. For this, many natural flower dyes have been used but only some of them are selected.

In DSSC, when we test the efficiencies at different times, T1 and T2, indeed we are measuring the contribution of the dye to pumping the electrons and increasing the efficiency, but in this type of DSSC, the efficiencies are low; maybe there is no cooperation between the excited dye electrons to promote the electrons from the valance band to CB of the TiO_2 semiconductor.

Although the present study hasn't been done for a long period, it makes several noteworthy contributions to the role of both spectra and environmental adaptation. The existence of UV peaks in dyes spectra means that the molecules of dyes have some resistivity for degradation as they can absorb the UV radiation and protecting the chromatic bond in a dye from broken and hence high stability as well. Accordingly, the dyes with high UV optical density absorbance peaks should be more

stable than those with low UV optical density absorbance peaks. This is valid for FF, HH, and AA in nursery flowers. However, for mountain flowers, the results add some other fact to this idea. All Gara flower dyes having high peaks, whether in UV or visible region, have high stability. This is because the flower that grows on the top of a mountain adapts itself to be alive with the existence of UV no matter how much the absorbance rate of UV. This adaptation enables the flower to get much more resistivity for degradation and hence supports more stability of the efficiency under severe conditions.

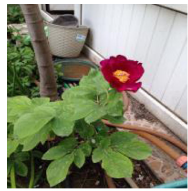
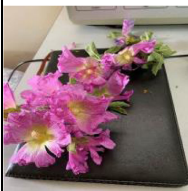





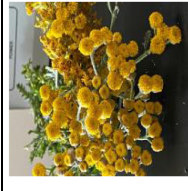

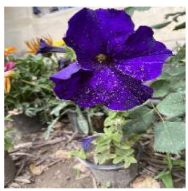
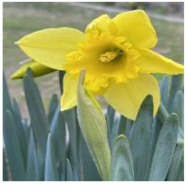

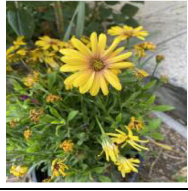


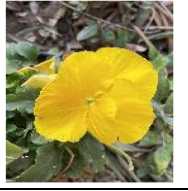
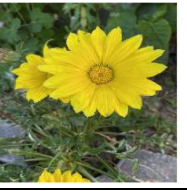
Statistically, this fact has been proved as there is no significant difference according to *P*-value for the efficiencies during a different period for all Gara mountain flowers that have high optical density whether in the UV region or visible region. So, the above two points are the reason why one should prefer mountain flower dyes over local flower dyes to get more stability of the DSSC. The small differences between the efficiencies at different periods are maybe due to the changing of the electrolyte concentration.

Regarding the efficiencies for all outdoor experiments that have been done at Duhok city (not on the mountain) which is only 410 m above sea level, it is found that all flowers dyes with most of their peaks at UV region have fewer efficiencies, like AD, YY, and XX in Gara Mountain flower and FF, HH, RR, and AA in nursery flowers, as shown in Fig 11. This is because of the low rate of UV radiation at the place of the experiment (Duhok city). In other words, it is believed that more UV radiation for such flowers might support more efficiency.

All flowers which have obvious peaks at the visible region in their spectra as in Fig. 12(a) and (b) give more efficiencies, like ZZ, VV, and TT in Gara mountain flowers and BB, II, CC, and SS in Duhok nursery flowers. This is because the rate of visible light is more than UV light at Duhok city.

It is obvious that the efficiencies were low in comparison to other workers. This might be due to the other components of these cells rather than the dye which we used, such as the lack of technology in the fabrication process besides the design of the cell which used only TiO₂ semiconductor as a working electrode, the photoelectrode, also it is not chemically treated using different precursor such as titanium (III) chloride (TiCl₃), titanium tetrachloride (TiCl₄), indium (III) and so on, that have been scientifically proven to help accelerate the electrons diffusion in TiO₂ film and preventing the recombination process [25]. Also, getting a certain thickness is very difficult especially with the manual doctor blading method that we depended on in this study; variation in several microns is huge when it comes to photovoltaic technology and has a significant effect on cell performance.

The idea of our research is to find good, stable, cheap, and easy for manufacturing solar cells with many natural dyes. The suitable natural dye which promotes electron from HOMO to LUMO and then to CB of the semiconductor of solar cell and increase the efficiency is our goal of this research. the next step is to find the structure of these dyes and with the help of the other parameters we may find the suitable new solar cell for industrial application.

<p>AD: <i>Paeonia officinalis</i> subsp. <i>Villosa</i></p> 	<p>YY: <i>Malva moschata</i> alba</p> 	<p>XX: <i>Hypericum thymopsis</i></p> 	<p>AB: <i>Helichrysum schwefellicht</i></p> 	<p>WW yellow: <i>Achillea filipendulina</i></p> 	<p>WW green leaves: <i>Achillea filipendulina</i></p> 
<p>ZZ: <i>Colutea arborescens</i>, Bladder senna -</p> 	<p>V V: <i>Tansy</i> (<i>Tanacetum vulgare</i>)</p> 	<p>TT: <i>primula veris</i> 'Cowslips'</p> 	<p>FF: <i>Petunia</i> 'Fanfare Deep Blue'</p> 	<p>HH: <i>Narcissus pseudonarcissus</i></p> 	<p>AA: <i>Calendula officinalis</i></p> 
<p>RR: <i>Osteospermum ecklonis</i></p> 	<p>CC: <i>Calendula</i> Pot Marigold</p> 	<p>BB: <i>Gazania rigens</i> Orange</p> 	<p>II: <i>Viola pedunculata</i> yellow pansy</p> 	<p>SS: <i>Gazania rigens</i> Yellow</p> 	

APPENDIX 1

SCIENTIFIC NAME [15]–[17], THE COD, AND THE PHOTO OF EACH FLOWER IN GARA MOUNTAIN AND NURSERY GROUPS FLOWERS

ACKNOWLEDGEMENT

The authors were particularly grateful for the assistance given by the Department of Physics, College of Science, University of Duhok. Also, their special thanks were extended to the staff of Dr Ahmed Family Pty Ltd., New South West, Australia for supplying them with SMU 2450-Keithley.

REFERENCES

- [1] S. Naman, "Photochemical cell of some dyes," *J. College Sci.*, vol. 29, no. 3, pp. 161–171, 1988.
- [2] S. A. Naman and A. S. R. Karim, "Efficiency of photogalvanic cells of dyes," *J. Sol. Energy Res.*, vol. 2, no. 1, pp. 31–41, 1984.
- [3] S. M. Aliwi, S. A. Naman and I. K. Al-Daghstani, "Photogalvanic effect of vanadium (III) bis(2,2'-bipyridyl) chloride and Fe(III) system," *Int. J. Sol. Cell*, vol. 18, pp. 85–91 1986.
- [4] A. Zakar, S. Naman, and S. M. Ahmed, "Improvement of the efficiency of dyed mono crystalline silicon solar cell by covering it with natural plants pigments," in *Proc. Int. Conf. Adv. Sci. Eng.*, 2019, pp. 230–235.
- [5] H. Gerischer, M. E. Michel-Beyerle, F. Rebertrost, and H. Tributsch, "Sensitization of charge injection into semiconductors with large band gap," *Electrochimica Acta.*, vol. 13, no. 6, pp. 1509–1515, 1968.
- [6] M. B. M. Abuiriban, "Dye-sensitized solar cell using natural dyes 'DSSCs,'" M.Sc. Thesis, Fac. Sci., Dept. Phys., Islamic Univ. Gaza, Gaza, Palestine, 2013.
- [7] M. Graetzel, R. A. J. Janssen, D. B. Mitzi, and E. H. Sargent, "Materials interface engineering for solution-processed photovoltaics," *Nature*, vol. 488, pp. 304–312, 2012.
- [8] M. Grätzel, "Dye-sensitized solar cells," *J. Photochem. Photobiol. C, Photochem. Rev.*, vol. 4, no. 2, pp. 145–153, 2003.
- [9] American Chemical Society, "Ultrathin, Dye-sensitized solar cells called most efficient to date," in *ScienceDaily*. Washington, DC, USA: American Chemical Society, Sep. 2006.
- [10] F. Gao *et al.*, "A new heteroleptic ruthenium sensitizer enhances the absorptivity of mesoporous titania film for a high efficiency dye-sensitized solar cell," *Chem. Commun.*, no. 23, pp. 2635–2637, 2008.
- [11] J. Burschka *et al.*, "Sequential deposition as a route to high-performance perovskite-sensitized solar cells," *Nature*, vol. 499, no. 7458, pp. 316–319, 2013.
- [12] B. O'Regan and M. Gratzel "A low-cost, high-efficiency solar cell based on dye-sensitized colloidal TiO₂ films," *Nature*, vol. 353, pp. 737–740, 1991.
- [13] S. Naman, "Energy conversion in the decay of triplet lumiflavin in the presence of Ferri- and Ferrocyanide," *Photochemistry Photobiol.*, vol. 47, no. 1, pp. 43–48, 1988.
- [14] P. F. Heelis *et al.*, "Acid—Base and redox properties of blepharismine photoreceptor pigments. A pulse radiolysis and flash photolysis study," *J. Photochemistry Photobiol. B: Biol.*, vol. 24, no. 1, pp. 41–45, 1994.
- [15] J. Lorenz, Ed., *Garden's Guide to Annuals and Perennials*, Lorenz Books. London, U.K.: Richard Bird Publisher, 2004.
- [16] R. Philips and M. Rix, Eds., *Early Perennials, the Garden Plant Series*. London, U.K.: Macmillan, 1991.
- [17] B. Bloembollen, Typical Dutch Bulbs & Concepts, Baltus Holland, Autumn 2020. [Online]. Available: www.bloembollen.com
- [18] B. A. Gregg, F. Pichot, S. Ferrere, and C. L. Fields, "Interfacial recombination processes in dye—sensitized solar cells and methods to passivate the interfaces" *J. Phys. Chem., B*, vol. 105, 2001, Art. no. 1422.
- [19] N. J. Cherepy, D. B. Liston, J. A. Lovejoy, H. Deng, and J. Z. Zhang, "Ultrafast studies of photoexcited electron dynamics in γ - and α -Fe₂O₃ semiconductor nanoparticles" *J. Phys. Chem., B*, vol. 102, 1998, Art. no. 770.
- [20] A. Kay, "Solar cells based on dye sensitized nanocrystalline TiO₂ electrodes" Ph.D. dissertation, Ecole Polytechnique Fédérale de Lausanne, Lausanne, Switzerland, 1994.
- [21] S. Ito *et al.*, "Fabrication of thin film dye sensitized solar cells with solar to electric power conversion efficiency over 10%," *Thin Solid Films*, vol. 516, pp. 4613–4619, 2008.
- [22] [Online]. Available: <https://www.sigmaaldrich.com/catalog/product/aldrich/791482?lang=en®ion=IQ>
- [23] M. Grätzel, "Dye-sensitized solar cells," *J. Photochemistry Photobiol. C: Photochemistry Rev.*, vol. 4, no. 2, pp. 145–153, 2003.
- [24] J. Wu *et al.*, "Counter electrodes in dye-sensitized solar cells," *Chem. Soc. Rev.*, vol. 46, 2017, Art. no. 5975.
- [25] N. Fadzilah *et al.*, "The effect of titanium (IV) chloride surface treatment to enhance charge transport and performance of dyesensitized solar cell," *Results Phys.*, vol. 15, 2019, Art. no. 102725.